

**ULTRAVIOLET CHARACTERIZATION OF FE-IMPREGNATED SILICA GELS AS ANALOGS FOR LUNAR SPACE WEATHERING.** K. R. Stockstill-Cahill<sup>1</sup>, J. T. S. Cahill<sup>1</sup> and C. A. Hibbitts<sup>1</sup>, <sup>1</sup>JHU-Applied Physics Laboratory, 11100 Johns Hopkins Rd., Laurel, MD 20723, Karen.Stockstill-Cahill@jhuapl.edu.

**Introduction:** The lunar surface and other airless planetary bodies undergo space weathering by micrometeorite bombardment and charged particle irradiation. On the Moon, space weathering produces submicroscopic iron (smFe<sup>0</sup>) particles that are deposited as either fine-grained rims on mineral grains or as larger particles within agglutinates. As a result of space weathering, visible-near infrared (Vis-NIR) spectra display an increase in the continuum slope (reddening), a reduction in albedo (darkening), and an attenuation of absorption features (shallowing) [1].

However, the manifestation of space weathering in lunar spectra imposed as a result of smFe<sup>0</sup> particle size is complex; for instance, larger smFe<sup>0</sup> particle sizes (<100-3000 nm) only darken, but do not redden the Vis-NIR spectra. Recent modeling techniques in the Vis-NIR have addressed this by applying Mie theory to account for the spectral effects of particle size variations in particle size.

This is all critical for accurately interpreting lunar surface maturity and composition but until now has not been explored at ultraviolet wavelengths in a similar manner to the Vis-NIR. The Lunar Reconnaissance Orbiter (LRO) features two ultraviolet instruments: the Lyman Alpha Mapping Project (LAMP) and the Lunar Reconnaissance Orbiter Camera Wide-Angle Camera (WAC). In order to examine the LRO ultraviolet data sets more effectively, we perform UV-NIR spectroscopy measurements and microscopy of lunar samples and analogs that previously provided guidance to visible and NIR [1].

**Methods:** Spectra were collected in the APL Laboratory for Spectroscopy under Planetary Environmental Conditions (LabSPEC). Spectra of the standard and sample are collected under high vacuum conditions (10<sup>-6</sup> to 10<sup>-7</sup> Torr). Ultraviolet (UV) data are collected using a McPherson monochromator (150-570 nm) using MgF<sub>2</sub> as the standard and a scintillating target in front a picometer. The monochromator and picometer are attached to chamber to enable far-UV data collection. Visible (Vis) data are collected using a Spectra Vista Corporation (SVC) HR-1024i point spectrometer (350-2500 nm) using MgF<sub>2</sub> as the standard. Infrared (IR) data are collected using a Bruker Vertex 70 lab FTIR (1.8-8 μm) using Au used as the standard. Both use a halogen light source with beam splitters (Quartz, KBr) and both spectrometers mounted outside chamber at dedicated ports that are 60° from the light source (i = 15°, e = 45°). The SVC and FTIR detectors are mounted on a linear

stage that allows us to toggle between the two spectrometers. A full spectrum, from UV (~150 nm) out to IR (~8 μm) is generated by combining three spectral ranges, scaled to the internally-calibrated SVC Vis spectrum.

**Samples:** This study utilizes silica gels of Noble et al. [1] which are impregnated with Fe<sup>0</sup> particles that vary in size from 5–200 nm. This study included four “series” of silica gels (SG2, SG6, SG25, SG50) with variable pore sizes that allowed different sizes of Fe<sup>0</sup> particles to be impregnated into each gel series in variable abundances (Table 1).

**Table 1:** Particle size series used in this study.

SG Series	Fe <sup>0</sup> Particle Sizes	Range of Fe <sup>0</sup> Abundance <sup>1</sup>
SG2	5 – 15 nm	0.02 – 1.21%
SG6	10 – 25 nm	0.02 – 0.30%
SG25	25 – 50 nm	0.02 – 0.94%
SG50	20 – 200 nm	0.03 – 1.89%

<sup>1</sup>Abundances included in this study

**Results:** Results for the smallest particle sizes (i.e., the SG2 series) show that spectra show the characteristic darkening and reddening within the Vis-NIR portion of the spectrum with increasing Fe<sup>0</sup> abundance. In Figure 1, spectra are displayed in rainbow order, from black (no Fe<sup>0</sup>) to purple (low Fe<sup>0</sup> abundance) to red (high Fe<sup>0</sup> abundance). It is apparent that as Fe<sup>0</sup> abundance increases, the spectra undergo darkening, shallowing, and reddening seen by [1].

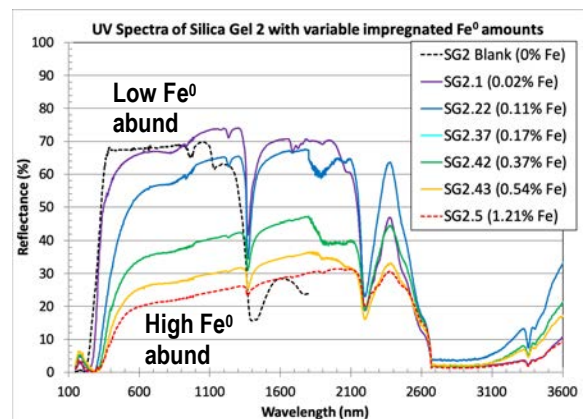


**Figure 1:** UV-NIR spectra of the SG2 series with variable smFe<sup>0</sup> abundances, which show the darkening and reddening effects of increasing smFe<sup>0</sup>.

(Note: Visible data shown as dashed lines in spectral plots were collected in an alternate set up and will not necessarily match overall albedo trends as other spectra. We plan to recollect these spectra at a future date.)

However, when we zoom in on the UV portion of the spectrum (Fig. 2), the inverse relationship between albedo and  $\text{Fe}^0$  abundance no longer exists. That is, samples containing a higher abundance of  $\text{Fe}^0$  (e.g., SG2.43, 0.54%  $\text{Fe}^0$ ) have higher albedos at wavelengths  $<220$  nm relative to samples with a lower abundance of  $\text{Fe}^0$  (e.g., SG2.1, 0.02%  $\text{Fe}^0$ ). SG2 series samples with intermediate  $\text{Fe}^0$  abundances follow this same trend (Fig. 2) so that there is positive correlation between  $\text{Fe}^0$  abundance and UV albedo. This transition occurs at lower wavelengths ( $\sim 250$  nm) than the WAC camera can observe ( $>320$  nm).

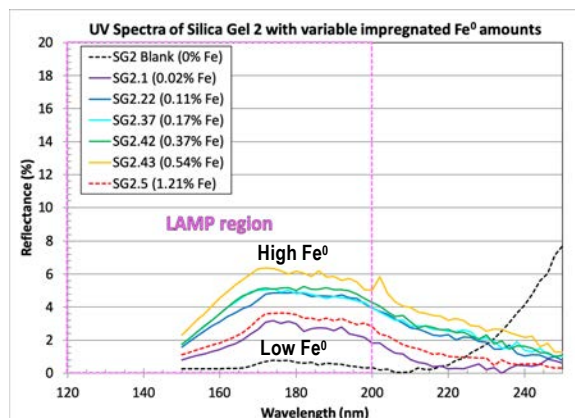


**Figure 2:** UV spectra for SG2 series with variable  $\text{Fe}^0$  abundances. Notice the increasing albedo and correlates with increasing  $\text{Fe}^0$  abundance. The spectral region covered by LAMP data is outlined by the violet dashed square.

Furthermore, when we look at the spectral behavior for larger particles sizes, the positive correlation between the UV albedo and  $\text{Fe}^0$  abundance progressively breaks down as the particle size increases. While the SG6 series also displays a positive correlation between  $\text{Fe}^0$  and UV albedo, it only maintains this at shorter wavelengths ( $<180$  nm). Indeed, the largest particle size sample series (SG25, SG50) display the inverse relationship between the albedo and the  $\text{Fe}^0$  abundance that is observed for the Vis-NIR (see Fig. 3).

**Summary:** The lunar UV albedo behaves very differently than the visible albedo [2]. Most minerals become opaque in UV even if bright in the visible. Furthermore, the mare/highlands contrast is minimal near MUV [3], and the mare UV reflectance is higher than highlands (Fig. 4). Indeed, the relative brightness between mare and highlands in the VNIR reverses at shorter wavelengths in the UV (Fig. 4).

The result of this study may suggest that the UV is most sensitive to the smallest  $\text{smFe}^0$  size fractions ( $<25$  nm) in or on a grain surface and not just sensitive to the finest regolith grain sizes as has been previously interpreted. With this information in hand, the UV albedo for

the Moon observed in LAMP data (Fig. 4) can be combined with Vis observations to better constrain the space weathering phases on the Moon. Specifically, in the mare where there is a larger Fe budget, a higher UV albedo and lower Vis albedo (relative to highlands) would be consistent with the  $\text{smFe}^0$  phase being dominated by the smallest particle sizes ( $<25$  nm). This work demonstrates the potential for UV observations to better constrain space weathering phases on airless bodies.

**Future and Ongoing Work:** We are working to verify the absence of this “UV reversal” within the larger particle sizes series (SG6, SG25, SG50) by collecting additional spectra within each series.

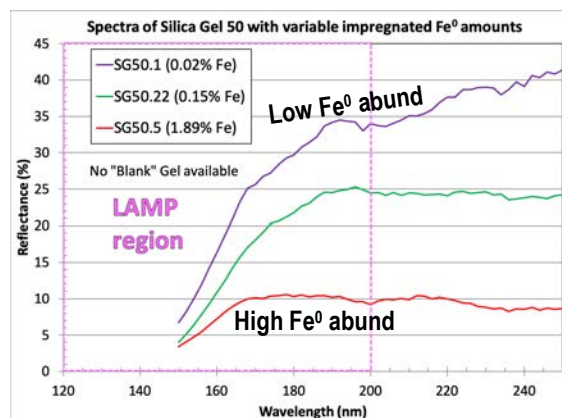


**Figure 3:** UV spectra for SG50 series with variable  $\text{smFe}^0$  abundances. Notice the decreasing albedo and correlates with increasing  $\text{Fe}^0$  abundance, as has been observed in the Vis-NIR.

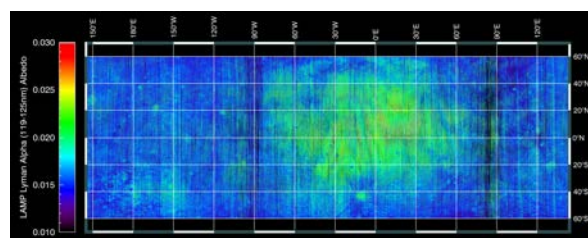


**Figure 4:** LAMP data of the Moon, showing the higher reflectance of the mare (greens) relative to the highlands (blues).

**References:** [1] Noble, S. K., C. M. Pieters, and L. P. Keller (2007) *Icarus*, 192, 629-642. [2] Henry, R. C., W. M. Fastie, R. L. Lucke, and B. W. Hapke (1976) *Moon*, 15, 51-65. [3] Henry, R. C., P. D. Feldman, J. W. Kruk, A. F. Davidsen, and S. T. Durrance (1995) *Astrophysics Journal*, 454, L69-L72.